ISSN 0021-3640, JETP Letters, 2019, Vol. 110, No. 11, pp. 750–754. © Pleiades Publishing, Inc., 2019.

MISCELLANEOUS

Thermophoresis-Assisted Microscale Magnus Effect in Optical Traps

M. N. Romodina[a], N. M. Shchelkunov[a], E. V. Lyubin[a], and A. A. Fedyanin[a, *]

[a] *Faculty of Physics, Moscow State University, Moscow, 119991 Russia*

**e-mail: fedyanin@nanolab.phys.msu.ru*

Received October 2, 2019; revised November 1, 2019; accepted November 6, 2019

The Magnus effect, commonly observed on the macroscale, has been considered to be negligible at the microfluidic limit. However, the thermophoretic effect at the microscale leads to a strong lift force that acts on the optically trapped and heated microparticles rotating in a liquid flow. This thermophoresis-assisted Magnus effect is experimentally observed and explained through the inhomogeneity of temperature distribution in the flow around the absorbing microparticles rotated by magnetic forces within the limit of ultralow Reynolds numbers.

DOI: 10.1134/S002136401923005X

The Magnus effect is a force acting on a rotating body in the flow of a liquid or gas and directed perpendicularly to the flow [1, 2]. There have been numerous experimental studies of the Magnus effect performed on the macroscale [3–8]. All of them are characterized by large or intermediate values of the Reynolds number Re, which is a dimensionless ratio between inertial and viscous forces in the system. For the range of $\mathrm{Re} \ll 1$, the Magnus force is considered to be negligible [9, 10]. For example, for a particle with a radius of 1 μm rotating with a frequency of 50 Hz and with a translational speed of 100 μm/s in a water, the Magnus force is as small as 10^{-16} N [11]. However, G. Chiparone et al. showed [12] that the Magnus force acting on the optically trapped microscopic droplets of a liquid crystal is by two orders of magnitude larger than the value predicted by the existing theoretical models. To explain this inconsistency between theory and experiment is an intriguing task since the difference could be a manifestation of the phenomenon observed on the microscale.

Microfluidics is characterized by large gradients of physical quantities, such as magnetic field or light power that are unobservable on the macroscale. These gradients are widely used, for example, in magnetic [13, 14] and optical [15, 16] tweezers. In addition, high gradients of temperature that can be achieved in a liquid result in the thermophoretic motion of microparticles [17]. Inhomogeneous heating in an optical trap can lead to a local temperature gradient and to the motion of the trapped microparticle through thermophoresis. Laser-induced heating has an effect even on the Brownian motion of particles [18].

Here we report on the experimental evidence of the lift force acting on the optically trapped magnetic microparticle rotating in a liquid flow. The lift force grows with the increase in local microparticle temperature, which is controlled by the trapping laser power. The correlation between the lift force and the heating of the microparticle in an optical trap indicates that the observed effect appears due to the thermophoretic forces that act on the heated microparticle rotated in the liquid flow. Using numerical simulations, we have shown that the heated microparticle rotating in the flow creates a temperature gradient around itself. The appearance of the temperature gradient can be explained by the displacement of the particle from the center of the optical trap during particle motion (see Fig. 1). The microparticle under the thermophoretic force moves in the direction opposite to the temperature gradient; therefore, the force has a component perpendicular to the flow. This is what constitutes the thermophoresis-assisted micro-scale Magnus effect.

In the present work, we studied the motion of magnetic microparticles in the optical trap. The microparticles were 3 μm in diameter and made from carboxyl-modified polystyrene with embedded 2–5% mass content magnetite nanograins (PMPEG-3.0, Kisker Biotech GmbH&Co). Approximately 40 μL of water suspension of microbeads at a concentration of 50 μg/mL was put into a hermetic chamber. A single microparticle was located 20 μm above the bottom of the chamber using the optical trap that was formed via focusing a diode laser beam with a wavelength of 980 nm through a high-numerical-aperture objective lens (NA = 1.3). The position of the optical trap along the *Ox* axis was controlled by an acousto-optical deflector, and the power of the light in the optical trap was set in the range from 6 to 44 mW. An additional laser with a 670 nm wavelength was used to detect microparticle displacements. The laser radiation was

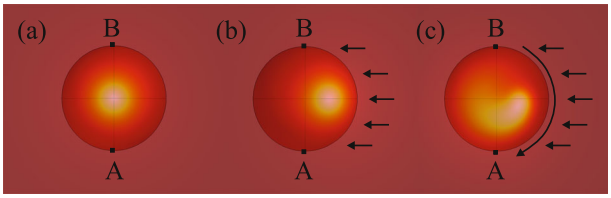

Fig. 1. (Color online) Temperature distribution in the optically trapped absorbing microparticle in the case of (a) a stationary particle in the absence of a liquid flow, (b) a stationary particle in the presence of a liquid flow, and (c) a rotating particle in a liquid flow. The lighter areas correspond to the higher temperature. The data are obtained using a numerical simulation of polystyrene 3-μm particle rotation with a frequency of $\Omega = 10^4$ Hz in water flowing with a speed of $V = 20$ μm/s.

scattered on the microparticle, collected with the help of a condenser and registered by a quadrant photodiode (QPD). The detection system was calibrated using the equipartition theorem for the Brownian fluctuations of a trapped microparticle [16]. To this end, the Brownian displacements of the microparticle in the stationary trap were measured for 100 s. The correlation functions of the microparticle displacements along the Ox and the Oy axes were analyzed [19], and the effective trap stiffnesses k_x and k_y were retrieved. The microparticle was rotated around the Oz axis after a 3.2 kA/m external magnetic field had been applied to the sample using the system of four electromagnets [20]. All measurements were performed at room temperature (25°C). However, it turned out that the magnetite nanograins embedded in the polystyrene microparticles slightly absorb the trapping light, which causes the temperatures of the microparticle and the surrounding liquid to increase. The effective temperature of the liquid around the trapped magnetic microparticle was obtained through analyzing the shift of the critical frequency of microparticle rotation in an external magnetic field [21]. The technical details of the experimental setup were described in [21–23].

In our experiments, the magnetic microparticle rotated at a rate up to 100 Hz. The trap position oscillated with an amplitude of up to 500 nm along the Ox-axis, with a frequency range of 2 to 20 Hz, causing linear particle motion with velocity that did not exceed 60 μm/s. The Reynolds number is

$$\mathrm{Re} = \rho U a/\eta, \tag{1}$$

where a is the radius of a particle, ρ is the density, and η is the viscosity of the fluid. For translational motion U is the particle velocity, and for rotational motion $U = 2\pi\Omega a$, where Ω is the frequency of particle rotation. Thereby, in our experiments, the translational Reynolds number is 10^{-4} and the rotational Reynolds number is 10^{-3} orders of magnitude. This is the case of ultralow Reynolds numbers [7, 11]. In the simulations, we are able to consider higher rotational speeds up to 10^4 Hz, which are not attainable in the experiment. Such values correspond to rotational Reynolds numbers up to 10^{-1}.

The displacements of the microparticle along the Ox and the Oy axes were measured by the oscillation of the optical trap along the Ox axis. It was averaged over 1000 oscillation periods to exclude the influence of the Brownian motion. Figure 2a shows the measured displacements of the particle along the Ox axis in the available registration range. The microparticle motion along the Ox axis is assumed to be sinusoidal, $X = x_0 \sin(2\pi ft)$, where x_0 and f stand for the amplitude and frequency of the microparticle oscillation along the Ox axis, respectively, and t is the time. The moment when the optical trap reaches the maximum speed along the Ox axis is marked by a dashed line. The rotation of the microparticle in the flow triggers the transversal force, which leads to microparticle displacement along the Oy axis. Assuming that this force linearly depends on the particle speed, it can be represented by the formula: $F_M(t) = F_M \cos(2\pi ft)$, where F_M is the amplitude of the transversal force. In the case of $\mathrm{Re} \ll 1$, the inertia is low enough to be neglected, and the displacement along the Oy axis can be written as follows [12]:

$$\begin{aligned} Y &= \frac{F_M}{\sqrt{k_y^2 + (2\pi f\gamma)^2}}\cos(2\pi ft + \varphi) \\ &= y_0 \cos(2\pi ft + \varphi), \end{aligned} \tag{2}$$

where $\gamma = 6\pi\eta a$ is the friction coefficient and $\varphi = \arctan(2\pi f\gamma/k)$ is the phase delay of the microparticle motion along the Oy axis [12]. As shown in Fig. 2b, the amplitude of the Y displacements is enhanced along with the gradually increased microparticle rotation rate. The maxima of the displacements are shifted along the Ox axes from the point of the optical trap maximal speed due to the delay in the particle response, which is caused by the viscosity of the liquid. The amplitude y_0 was found using synchronous detection to minimize the influence of thermal noise that was induced by the particle Brownian motion.

The value of the transversal force was estimated as follows:

$$F_M = y_0\sqrt{k_y^2 + (2\pi f\gamma)^2}. \tag{3}$$

Its dependencies on the microparticle rotation rate and linear speed are shown in Figs. 2c and 2d, respectively, and it is proportional to them both. In the represented data, the force was averaged across seven samples with different microparticles, and the error bars correspond to statistical errors. The linear dependence of the transversal force on these parameters is typical of the Magnus effect.

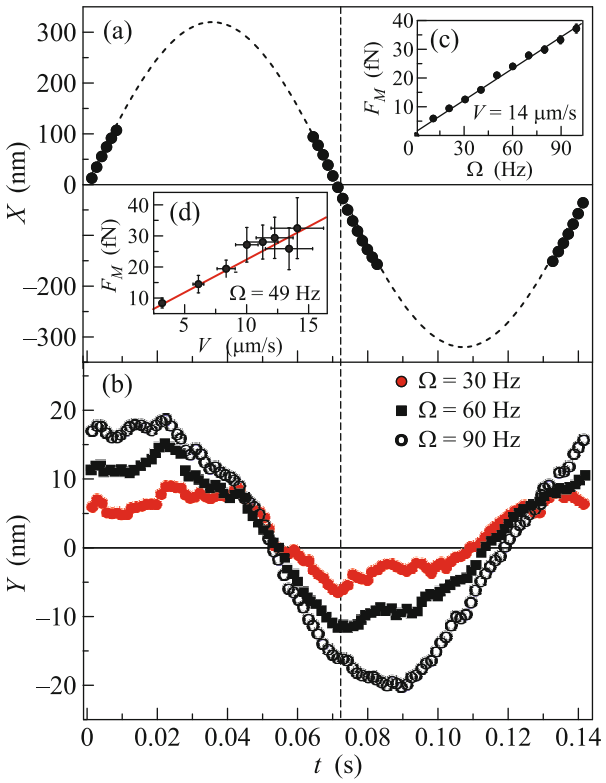

Fig. 2. (Color online) Averaged microparticle displacements along the (a) *Ox* and (b) *Oy* axes measured at different microparticle rotation rates. The dashed curve indicates the estimated trajectory of the particle along the *Ox* axis (a). Thermophoretic Magnus force versus (c) the rotation rate of the microparticle and (d) the microparticle linear speed. The amplitude of the trap oscillation was $A = 500$ nm, and the laser power inside the trap was $P = 20$ mW.

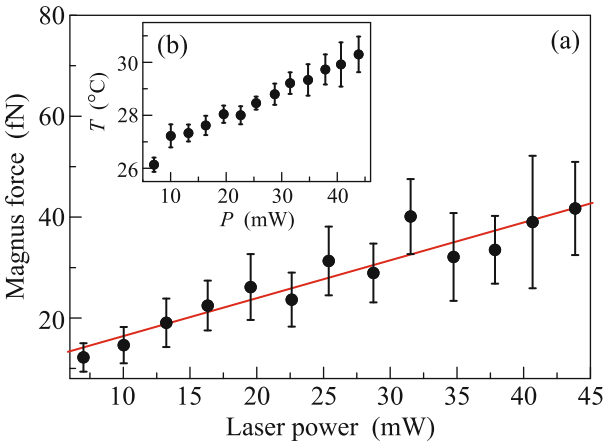

Fig. 3. (Color online) (a) Thermophoresis-assisted Magnus force dependence on the laser power in the optical trap. The oscillation frequency $f = 9$ Hz, the amplitude of the trap oscillation $A = 200$ nm, and the microparticle rotation rate $\Omega = 50$ Hz. (b) Effective temperature of the microparticle surface versus the trapping laser power.

The absorption of laser radiation leads to heating of the trapped microparticles. The dependence of the transversal force on the laser light power inside the trap is shown in Fig. 3a. As the laser power increases, the force grows significantly, allowing one to suggest that heating plays an important role in the effect. The effective temperature of the liquid around the trapped magnetic microparticle grows linearly along with the light power inside the trap (see Fig. 3b). The studied effect could arise from the local non-uniform heating and the appearance of temperature difference on the opposite sides of a trapped microparticle. The observed high values of the Magnus force can account for thermophoresis, also called thermal diffusion, which moves microscopic particles along temperature gradients [24–26].

Thus, the thermophoresis-assisted Magnus force is caused by temperature difference on opposite sides of the microparticle. The difference appears due to the displacement of the absorbing microparticle from the center of the optical trap during its motion in the liquid flow. The temperature distribution around the optically trapped microparticle rotating in the liquid flow was obtained by numerical solutions of the heat equation, solved using the finite element method. To illustrate the key processes of the studied phenomena, we calculated the temperature distribution (Fig. 1) for both the case of a high rotational frequency of 3-μm particle, $\Omega = 10^4$ Hz and the flow velocity $V = 20$ μm/s. When a particle the size of several micrometers was placed in an optical trap the size of 1 μm, the center of the particle is heated (Fig. 1a). Under the impact of the flow, the particle is displaced from the center of the trap and the temperature distribution in the microparticle becomes asymmetrical (Fig. 1b). When the microparticle rotates in the liquid flow, the heated area of the microparticle moves along a circular path and cools due to the contact with the liquid, which creates a non-uniform distribution of the particle temperature (Fig. 1c). In the simulation, the product of the optical power and the absorption of the particle is within the fitting parameter, which is consistent with the experimental average temperature of the medium near the particle. The case of high rotational speed is depicted for good visibility of key mechanism of the process, which is the shift of the hot region inside the particle. The shift is still retained qualitatively at lower rotational speeds. For the particle rotation rate of 50 Hz and the liquid flow speed of 25 μm/s, the temperature difference at the points A and B is $\Delta T = 0.12$°C, which corresponds to the gradient of 0.04°C/μm.

The calculated dependencies of ΔT on the microparticle rotation rate and flow velocity are shown in Fig. 4. ΔT rises in the range of flow velocity from 0 to 25 μm/s. This range corresponds to the experimental values, as the measured force is also rising. At flow

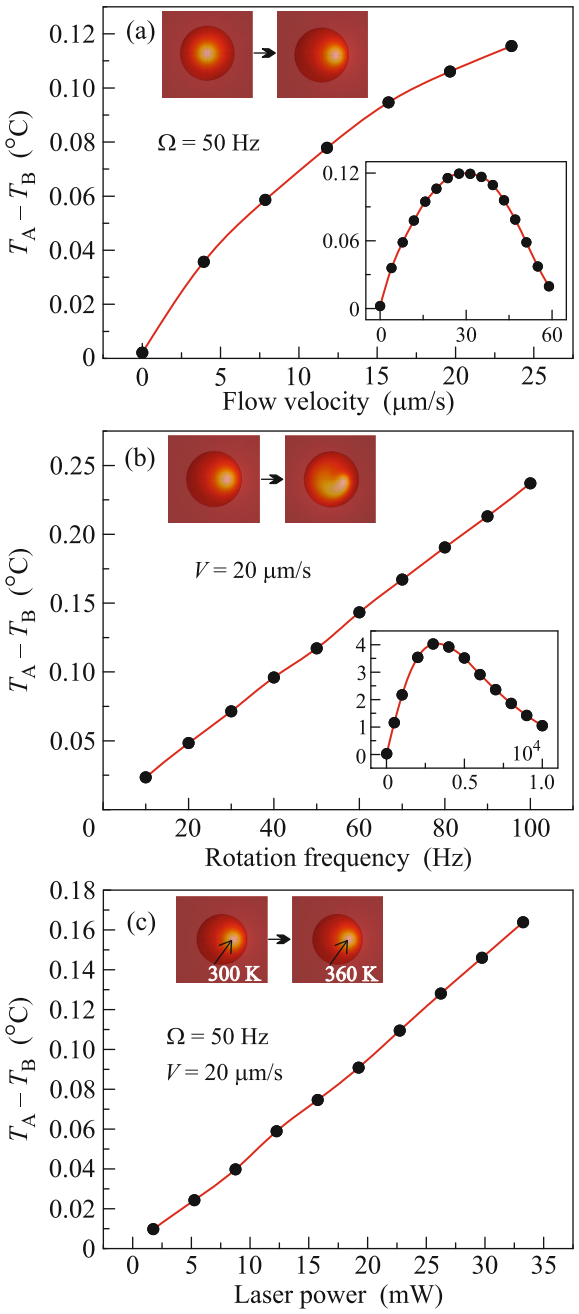

Fig. 4. (Color online) Temperature difference between the left (point A, Fig. 1) and the right (point B) sides of the particle, obtained using numerical simulation: (a) is the dependence on liquid flow velocity, inset is the case of high values of liquid flow velocity; (b) is the dependence on the frequency of microparticle rotation, inset is the case of high values of rotation frequency; (c) is the dependence on laser power.

speed above 30 μm/s, the spot of the laser trap exceeds the microparticle surface; it reduces the microparticle heating and leads to the decrease in temperature difference. The dependence of ΔT on the microparticle rotation rate grew linearly from 0 to 10^3 Hz, which includes the experimentally studied values of microparticle rotation rates. At the frequencies above 3×10^4 Hz, ΔT decreases because the speed of microparticle rotation becomes higher than the speed of heat transfer to liquid. The dependence on the laser power also grew linearly (Fig. 4c) in accordance with the data for the experimentally measured force (Fig. 3a).

The coupling coefficient S_M between the temperature distribution and the force acting on the particle can be estimated using the closest analogue—the equation for the thermophoretic force in the case of a uniform temperature gradient:

$$\mathbf{F}_{\text{thermo}} = -k_B T S_T \nabla T, \tag{4}$$

where k_B is the Boltzmann constant, T is the temperature of the liquid, and S_T is the Soret coefficient.

We estimated the value of S_M from Eq. (4), substituting it with S_T and using the experimental data for $\mathbf{F}_{\text{thermo}} = 25$ fN (see Fig. 3a), calculated the value of $\nabla T = 0.04$°C/μm (see Fig. 4c) and obtained the value of $S_M \approx 150$ K^{-1}. While in the case with a uniform gradient, the coefficient $S_T \approx 18$ K^{-1} for a similar system [27].

There is no generally accepted theoretical framework for the Soret coefficient [28], but it is known that S_T strongly depends on the particle-solvent interface, and therefore has a highly specific surface chemistry, such as the degree of surface ionization, or the amount of residual surfactant used in emulsion. Moreover, it strongly depends on temperature [27]. In the case scrutinized here, the temperature distribution on the surface of the particle is strongly nonuniform, and the temperature inside the particle is much higher than it is on the surface, which can significantly affect the charge of the particle and the degree of surface ionization.

Summarizing, in the present study we have directly measured the thermophoresis-assisted Magnus force that acts on the optically trapped magnetic microparticles rotating in a liquid flow. The lift force arises from to the inhomogeneity of the temperature distribution around the microparticle, induced by its rotation in the liquid flow. The growth of the Magnus force with the increase in the trapping laser power reveals the key role of heating of the trapped microparticle. The measured force is valued in the same order of magnitude as the theoretical estimation based on the simulation of temperature distribution around optically trapped microparticle. The information gleaned from considering the thermophoresis-assisted Magnus effect for all these systems may be promising for a variety of biological and micro-rheological studies. For instance, it may be relevant in testing of the mechanical properties of macromolecules, living cells and micro-droplets shells.

FUNDING

This work was supported by the Russian Ministry of Education and Science (contract no. 14.W03.31.0008), by the Russian Science Foundation (project no. 15-02-00065 for the experiment and project no. 18-72-00247 for calculations), by the Russian Foundation for Basic Research (project no. 18-32-20217), and in part by the Quantum Technology Center, Moscow State University.

REFERENCES

1. L. Prandtl, Naturwissensch. **13**, 93 (1925).
2. G. Magnus, Ann. Phys. **164**, 1 (1853).
3. J. M. Davies, J. Appl. Phys. **20**, 821 (1948).
4. J. W. Maccoll, J. Aeronaut. Soc. **32**, 777 (1928).
5. H. M. Barkla and L. J. Auchterlonie, J. Fluid Mech. **47**, 437 (1971).
6. R. Eichhorn and S. Small, J. Fluid Mech. **20**, 513 (1964).
7. Yu. Tsuji, Yo. Morikawa, and O. Mizuno, J. Fluids Eng. **107**, 484 (1985).
8. B. Oesterle and T. B. Dinh, Exp. Fluids **25**, 16 (1998).
9. S. Martin, M. Reichert, H. Stark, and T. Gisler, Phys. Rev. Lett. **97**, 248301 (2006).
10. G. Volpe and D. Petrov, Phys. Rev. Lett. **97**, 210603 (2006).
11. S. I. Rubinow and J. B. Keller, J. Fluid Mech. **11**, 447 (1961).
12. G. Cipparrone, R. J. Hernandez, P. Pagliusi, and C. Provenzano, Phys. Rev. A **84**, 015802 (2011).
13. K. C. Neuman and A. Nagy, Nat. Methods **5**, 491 (2008).
14. I. De Vlaminck and C. Dekker, Ann. Rev. Biophys. **41**, 453 (2012).
15. A. Ashkin, J. M. Dziedzic, J. E. Bjorkholm, and S. Chu, Opt. Lett. **5**, 288 (1986).
16. K. C. Neuman and S. M. Block, Rev. Sci. Instrum. **75**, 2787 (2004).
17. R. Piazza and A. Parola, J. Phys.: Condens. Matter **20**, 153102 (2008).
18. E. J. G. Peterman, F. Gittes, and Ch. F. Schmidt, Biophys. J. **84**, 1308 (2003).
19. J.-C. Meiners and S. R. Quake, Phys. Rev. Lett. **82**, 2211 (1999).
20. M. N. Skryabina, E. V. Lyubin, M. D. Khokhlova, and A. A. Fedyanin, JETP Lett. **95**, 560 (2012).
21. M. N. Romodina, E. V. Lyubin, and A. A. Fedyanin, Sci. Rep. **6**, 21212 (2016).
22. E. V. Lyubin, M. D. Khokhlova, M. N. Skryabina, and A. A. Fedyanin, J. Biomed. Opt. **17**, 101510 (2012).
23. D. A. Shilkin, E. V. Lyubin, I. V. Soboleva, and A. A. Fedyanin, JETP Lett. **98**, 644 (2013).
24. T. L. Bergman and F. P. Incropera, *Introduction to Heat Transfer* (Wiley, Hoboken, NJ, 2011).
25. R. Piazza, Soft Matter **4**, 1740 (2008).
26. K. I. Morozov, J. Exp. Theor. Phys. **88**, 944 (1999).
27. M. Braibanti, D. Vigolo, and R. Piazza, Phys. Rev. Lett. **100**, 108303 (2008).
28. A. Wurger, C.R. Mec. **341**, 438 (2013).